S Minjoli, G B Saturnino, J Udby Blicher, C J Stagg, H R Siebner, A Antunes, A Thielscher

The impact of large structural brain changes in chronic stroke patients on the electric field caused by transcranial brain stimulation

Supplementary Material

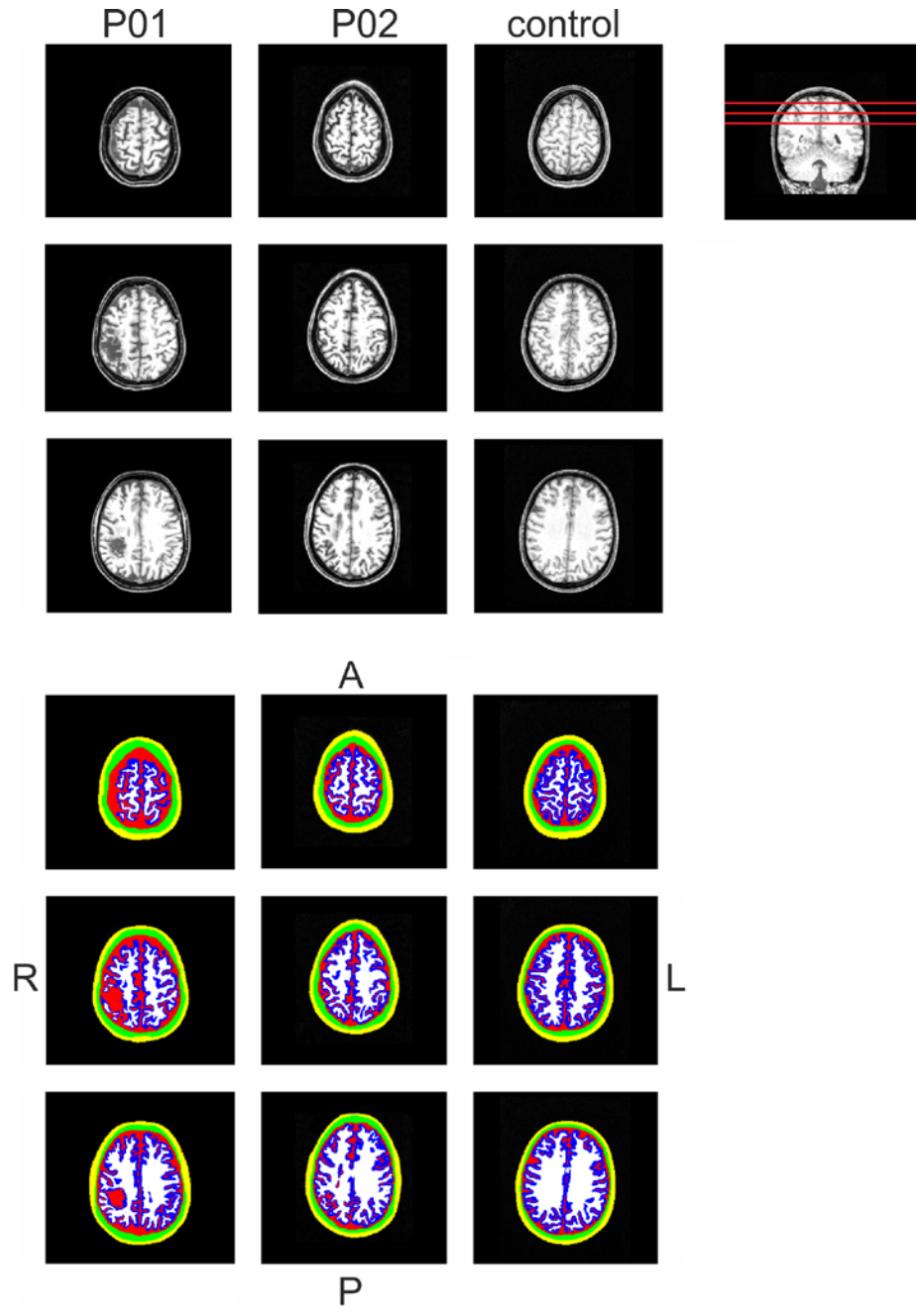

Figure S1: Horizontal cuts through the T1w images (top) and the final segmentations (bottom). The images are in radiological convention. Their positions are indicated as red lines in the coronal slice

of the control subject (top right). The colours correspond to skin (yellow), skull (green), CSF (red), GM (blue) and WM (white).

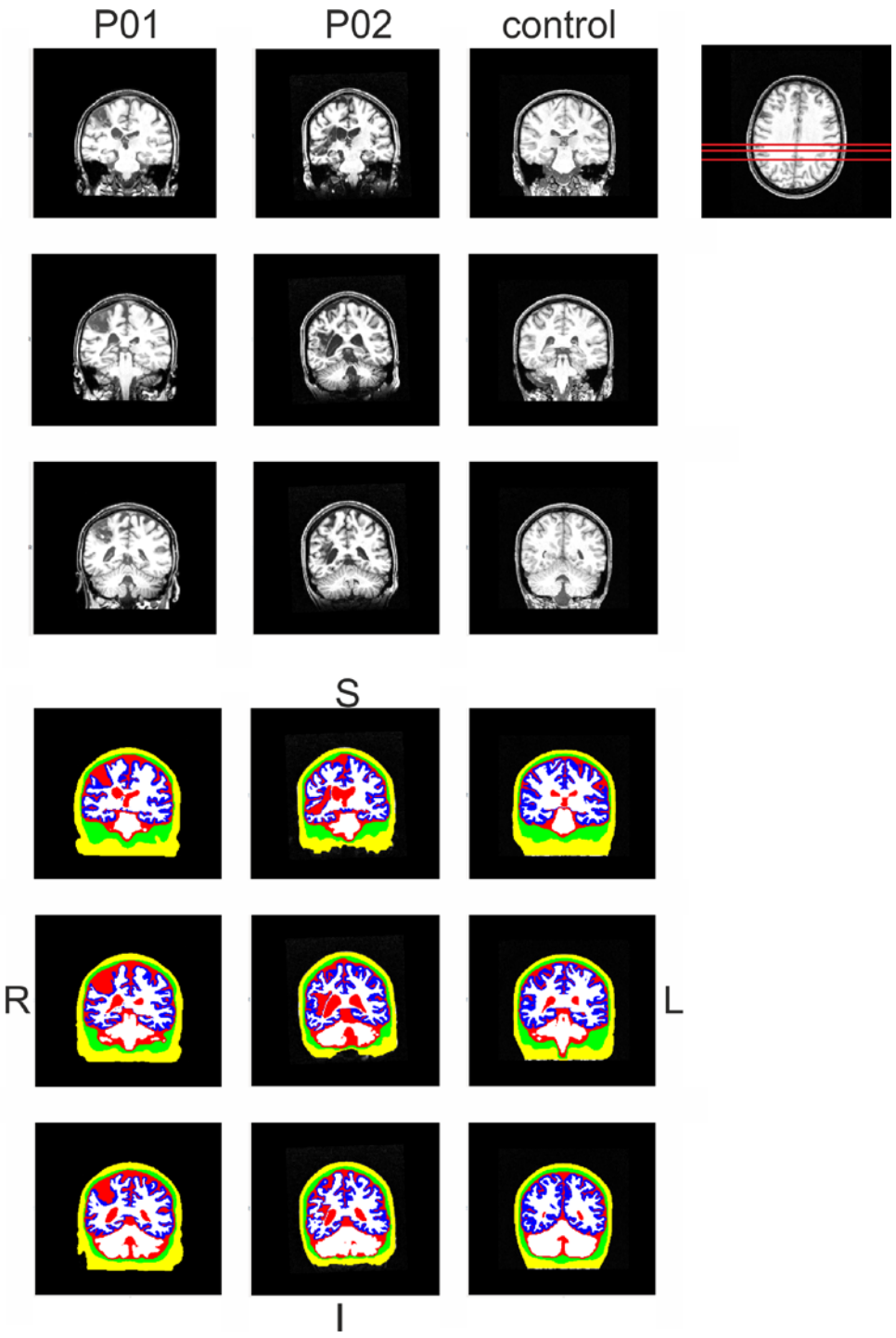

Figure S2: Coronal cuts through the T1w images (top) and the final segmentations (bottom). The images are in radiological convention. Their positions are indicated as red lines in the horizontal slice of the control subject (top right). The colours correspond to skin (yellow), skull (green), CSF (red), GM (blue) and WM (white).

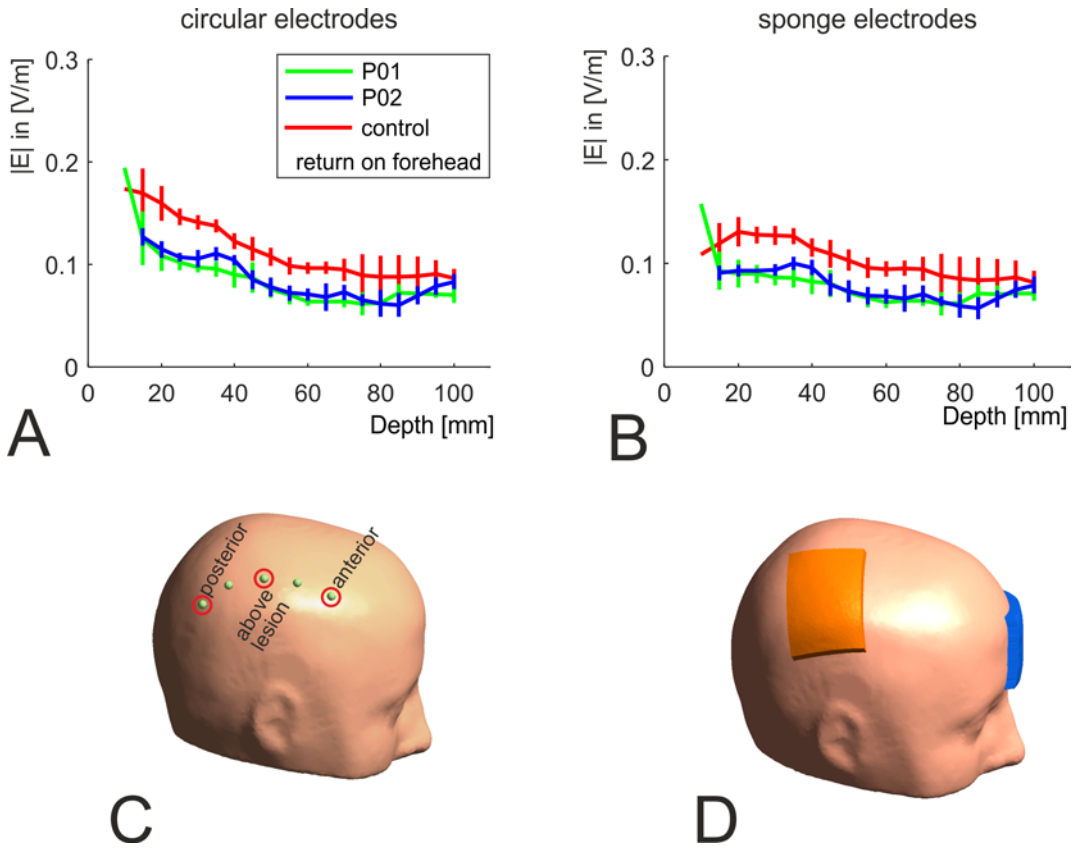

Figure S3: A) Depth profiles for TDCS, assessed for the circular electrodes used in the main part of the paper. The profiles were averaged across the three electrode positions shown in subfigure C. B) Depth profiles for TDCS, assessed for rectangular electrodes. The profiles were averaged across the three electrode positions shown in subfigure C. The electrodes had an area of 50x70 mm and a height of 6mm high. Their conductivity was modelled as 1.5 S/m. They contained an embedded rubber layer (area 30x50 mm, 1 mm high, conductivity 27 S/m). The connector to the cable was modelled to be placed on the top centre of the rubber layer. C) The red circles highlight the electrode positions used for the comparison of circular versus sponge electrodes. D) Exemplary visualization of the orientation of the rectangular sponge electrodes.

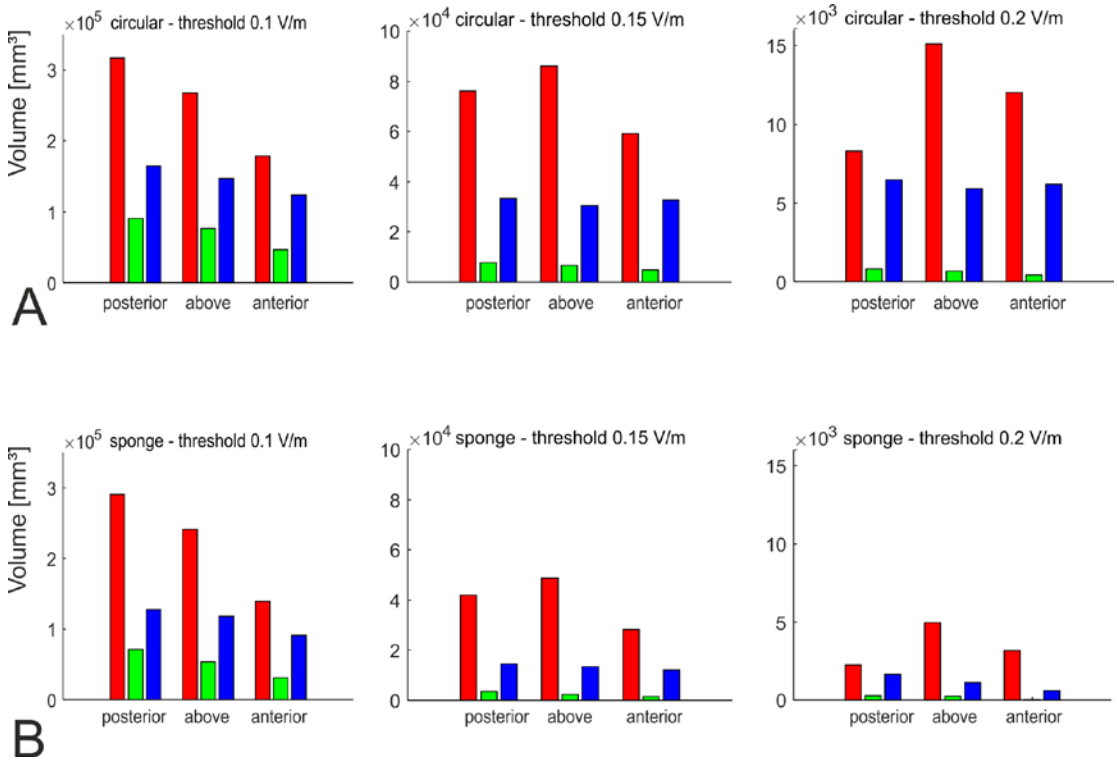

Figure S4: Grey matter volumes in which the field strength is above the threshold indicated in the figure titles (green: P01; blue: P02; red: healthy control). A) Results for the circular electrodes. B) Results for the sponge electrodes. The difference between the lesion models and the healthy control is stable across thresholds and occurs for both electrode types. On average, the sponge electrodes inject slightly weaker fields than the circular electrodes (indicated by the lower volumes for the threshold of 0.2 V/m). A likely reason is the more diffuse injection of the fields caused by the larger area of the sponge electrodes.

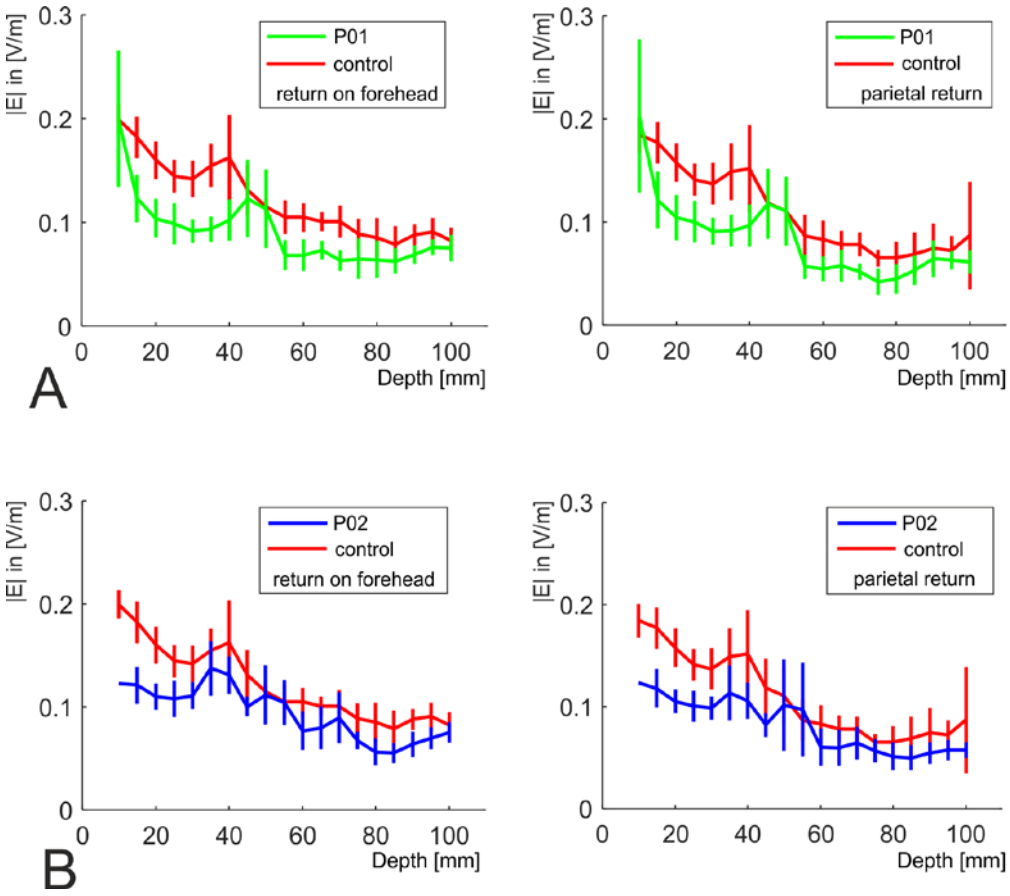

Figure S5: Depth profiles for TDCS, assessed for the circular electrodes used in the main part of the paper, but reassessed in cylinders of 30 mm diameter rather than 80 mm. In the main part of the paper, 30 mm was used for TMS (Fig. 2) while 80 mm was used for tDCS (Fig. 5). The profiles were averaged across the nine electrode positions shown in Fig. 1D. While the results show more variation due to small diameters than the original results (indicated by the higher standard deviations here compared to Fig. 5), the general differences between the head models are stable. However, it is interesting to note that the same field strength is reached at a few particular depth intervals in the patient head models compared to the healthy control. For example, visual inspection revealed that the increased field strengths in the depths of 45 mm for P01 corresponds to "hot spots" in the tissue between the lesion and the ventricles that occurred for some of the electrode positions (see Fig. 7C). This effect was "averaged out" when basing the depth profiles on cylinders with 80 mm diameter.